INL/JOU-24-76241-Revision-1



# Droplet entrainment in steam supply system of water-cooled small modular reactors: experiment and modeling approaches

December 2024

Kenneth Lee Fossum, Palash Kumar Bhowmik

Changing the World's Energy Future


*INL is a U.S. Department of Energy National Laboratory operated by Battelle Energy Alliance, LLC*

**DISCLAIMER**

This information was prepared as an account of work sponsored by an agency of the U.S. Government. Neither the U.S. Government nor any agency thereof, nor any of their employees, makes any warranty, expressed or implied, or assumes any legal liability or responsibility for the accuracy, completeness, or usefulness, of any information, apparatus, product, or process disclosed, or represents that its use would not infringe privately owned rights. References herein to any specific commercial product, process, or service by trade name, trade mark, manufacturer, or otherwise, does not necessarily constitute or imply its endorsement, recommendation, or favoring by the U.S. Government or any agency thereof. The views and opinions of authors expressed herein do not necessarily state or reflect those of the U.S. Government or any agency thereof.

INL/JOU-24-76241-Revision-1

# Droplet entrainment in steam supply system of water-cooled small modular reactors: experiment and modeling approaches

**Kenneth Lee Fossum, Palash Kumar Bhowmik**

**December 2024**

**Idaho National Laboratory**
**Idaho Falls, Idaho 83415**

**http://www.inl.gov**

**Prepared for the**
**U.S. Department of Energy**
**Under DOE Idaho Operations Office**
**Contract DE-AC07-05ID14517**

Journal of
*Nuclear Engineering*

MDPI

*Article*

# Droplet Entrainment in Steam Supply System of Water-Cooled Small Modular Reactors: Experiment and Modeling Approaches

**Kenneth Lee Fossum *, Palash Kumar Bhowmik and Piyush Sabharwall**

Thermal Fluid Systems Methods and Analysis Department, Idaho National Laboratory, 1955 Fremont Avenue, Idaho Falls, ID 83415-2209, USA; palashkumar.bhowmik@inl.gov (P.K.B.)
* Correspondence: kenneth.fossum@inl.gov

**Abstract:** Droplet entrainment in steam-flow is a prominent phenomenon that needs adequate safety and risk analysis of postulated transient and accident scenarios—including experimental investigation and representative modeling and simulation (M&S)—for small modular reactor (SMR) system design and demonstration. This study identifies knowledge gaps by evaluating experimental and computational fluid dynamics modeling approaches to support early-stage reactor system design, testing, and model evaluation. Previous studies reported in the literature for steam-flow entrainment primarily focused on gigawatt capacity pressurized water reactor (PWR) systems. However, entrainment phenomena are even more prominent for PWR-type SMRs due to their more compact integrated designs, which need further research and development. To fill the research gaps, this study provides insight by specifying the phenomena of interest by leveraging the lessons learned from past research, adopting advanced M&S techniques and advanced instrumentation and control. The findings and recommendations are applicable for evaluating steam-flow entrainment models and for designing integral effect test and separate effect test facilities for gaining reactor design approvals.

**Keywords:** small modular reactor; steam supply system; droplet entrainment; experiment; modeling and simulation

check for updates

**Citation:** Fossum, K.L.; Bhowmik, P.K.; Sabharwall, P. Droplet Entrainment in Steam Supply System of Water-Cooled Small Modular Reactors: Experiment and Modeling Approaches. *J. Nucl. Eng.* **2024**, *5*, 563–583. https://doi.org/10.3390/jne5040035

Academic Editor: Dan Gabriel Cacuci

Received: 16 September 2024
Revised: 10 November 2024
Accepted: 27 November 2024
Published: 12 December 2024

**Copyright:** © 2024 by the authors. Licensee MDPI, Basel, Switzerland. This article is an open access article distributed under the terms and conditions of the Creative Commons Attribution (CC BY) license (https://creativecommons.org/licenses/by/4.0/).

## 1. Introduction

Small modular reactors (SMRs) are attracting the attention of nuclear skeptics, scientists, policymakers, and investors as one of the next major frontiers of nuclear energy technology. With government and private USD totaling well into the tens of billions for research and licensing efforts, technological advancement and excitement is building quickly toward a new nuclear future. These smaller units, usually classified by having an electrical output of 300 megawatts (MW) or less [1], are designed to be more rapidly deployed while also having improved safety over existing large-scale nuclear power plants (NPPs).

A significant portion of SMR safety improvements come from their featuring passive systems as integral components of both normal power operation and accident response, which are not reliant on operator action for initiation, nor reliant on alternating current electric power, or both. A major challenge to incorporating passive elements into a design is that this has not been the norm for most commercial nuclear reactors. The hurdle of proof is made tall by regulators for exactly this reason. It is well-established that the U.S. Nuclear Regulatory Commission (NRC) can be convinced that redundant pumps will not both suddenly fail to perform their function simultaneously; it is a whole new challenge for passive principles to stand up to every design-basis accident while also providing defense-in-depth to beyond design-basis accidents without compromising on safety. While an abundance of empirical data exists for operating commercial reactors, SMRs require further effort to build empirical knowledge of their safety envelope. One of the phenomena not well-understood in relation to SMRs is droplet entrainment by steam.

Entrainment is a process where liquid drops are carried by vapor. This phenomenon is illustrated in Figure 1. The term can also be called droplet entrainment or liquid entrainment. One of the simplest numerical representations is given in Equation (1) as the ratio of entrained droplet mass flow rate to total liquid flow rate. Another numerical way to interpret entrainment is with void fraction, seen in Equation (2), which is the fraction of the volume or flow cross-section occupied by the gas phase. A common way to measure and derive entrainment is using a void fraction as a substitute, which can be accurate if the void fraction is 1.0 without any entrainment occurring.

$$e = \frac{\dot{m}_{le}}{\dot{m}_l} \tag{1}$$

where

$e$ = entrained liquid ratio
$\dot{m}_{le}$ = droplet mass flow rate
$\dot{m}_l$ = total liquid mass flow rate

$$\alpha = \frac{A_v}{A_{v+l}} \tag{2}$$

where

$\alpha$ = void fraction
$A_v$ = flow area occupied by vapor
$A_{v+l}$ = total flow area of vapor and liquid

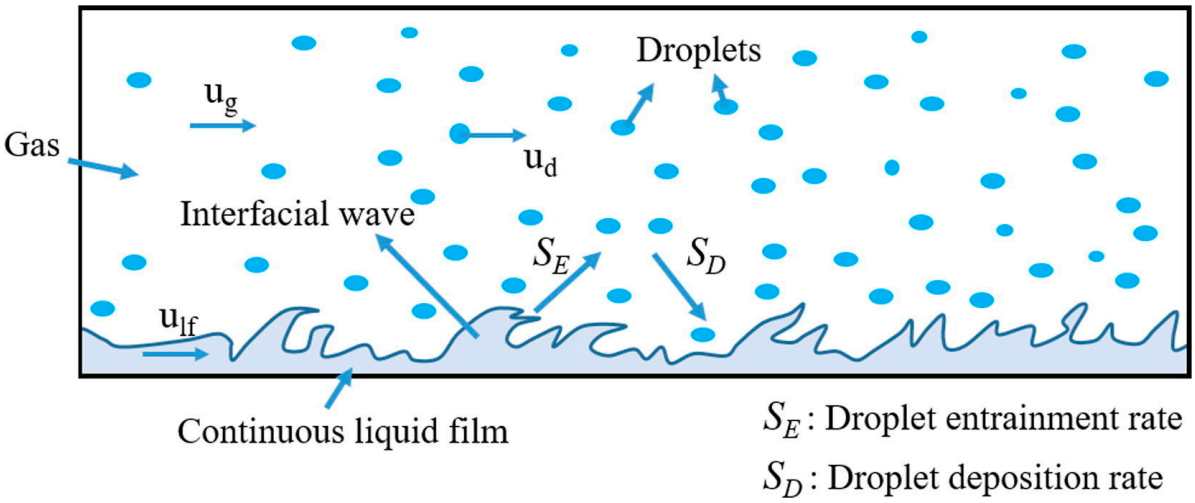


**Figure 1.** Droplets carried in the gas phase of two-phase flow is called entrainment. Reproduced with permission from [2]. Copyright Elsevier, 2019.

This phenomenon can be an important consideration for anything from public health and virus dispersal by a sneeze [3] to NPP operational safety. One aspect of the phenomenon in power plants results in a saturated two-phase mixture in a steam line rather than the typical single phase of superheated steam. Certain accident scenarios, bypassing normal operation, will render moisture separator components unable to mitigate this occurrence. These scenarios will differ between pressurized water reactors (PWRs) and boiling water reactors (BWRs), but a main steam line break (MSLB) is one such example that would apply to all light water reactor (LWR) designs. When the steam line is ruptured, depressurization of the loop will result. When this occurs, the density of the fluid and saturation temperature decrease in tandem. As fluid is rapidly exiting the break, an increasing amount of liquid is boiled into steam due to the changing saturation conditions. This boiling and the fluid blowdown through the break are violent processes that do not allow liquid to settle out of

the vapor flow. In an energy balance sense, the liquid leaving the system with the steam could be seen as positive because of the high-energy density of the liquid. However, as the liquid leaves the break and enters a lower-pressure environment, it rapidly flashes to steam and expands. If the break has occurred inside containment, there is now high-pressure steam and liquid flashing to steam injected inside an enclosed volume that must cope with the pressure rise. While the depressurization of the system makes water injection easier for cooling the core, the expanding fluid is challenging the last fission product barrier remaining to protect the environment and public from harmful radiation doses. The NPP should have safety systems in place, or sufficient analysis if it is reliant on passive processes, to mitigate or cope with this pressure rise without exceeding containment design limits of pressure and temperature. This safety parameter is of particular concern for SMRs as they are designed to have much smaller containment volumes than their large-scale counterparts.

For a PWR-specific accident that could cause entrainment and is quite common, a steam generator tube rupture (SGTR) would not directly challenge the containment structure but could bypass the fission product retention aspect of containment. In this scenario, the hotter, higher-pressure primary fluid enters the steam generator through the broken heat transfer tubes. Unless detected, the steam generator could overfill and allow water to be entrained in the main steam line (MSL) flow. While entrainment is not the main concern in these accidents, it would be a phenomenon in need of investigation. At the SMR scale, the more compact design of components like the steam generator will mean that less liquid will need to be leaked from a steam generator tube to reach the point of overfill. In BWRs, entrainment would occur if core power approached and bypassed the critical heat flux (CHF) limit of the fuel rods. Dryout of the fuel rods occurs as droplets are entrained in the steam flow and moved away from contact with the fuel cladding [4]. This is of paramount importance in accident analysis because if CHF has been reached, the fuel and cladding can rapidly overheat, risking failure and a severe accident. The more compact components like the core or steam generator could mean that accident conditions develop quicker. Specific investigation of the important phenomena with properly scaled integral effect test (IET) facilities is paramount to answer the questions a thorough licensing process will require paying attention to.

During normal power operation, a steam generator will almost completely vaporize the liquid present before entering the MSL. However, during a depressurization transient or incident causing a raised liquid level in the steam generator, a significant amount of liquid can remain in the steam flow. The role of this study is to outline the difference in entrainment incidence and impact in an SMR power plant as compared to a large-scale NPP as well as highlight the gaps in the state of knowledge (SOK) for the entrainment phenomena to suggest an approach for improvement.

The magnitude of entrainment in pipe flow is largely determined by the two-phase flow regime, and early work from [5] showed the dependence of the onset of entrainment on the liquid Reynold's number. This is different than entrainment resulting from pool boiling in a vessel, which is dependent on droplet proximity to the vessel exit, where gas superficial velocity is highest [6]. Two-phase flow is a complicated fluid mechanics problem, as well as heat transfer interaction in the case of steam and water. Many modeling approaches thus far have used air and water to simulate a two-phase steam flow, which ignores the heat transfer component. These are useful for validating computational fluid dynamics (CFD) codes and will be reviewed in this study alongside the steam/water tests in an analysis of the knowledge gaps that still exist in this important phenomenon. A discussion of future experimental research and recommended instrumentation strategies will also be covered in this study.

## 2. Physics Phenomena and POI

Reactor system thermal hydraulics experiments, in addition to modeling and simulation (M&S), greatly depend on the physics phenomena and phenomenon of interest

(POI), and steam entrainment is not an exception. Entrainment phenomena in the reactor system MSL of either a PWR or a BWR exist in two-phase flow (i.e., steam and entrained liquid/condensate), while the associated and important physics phenomena are (a) two-phase flow regimes, (b) conservations of energy and momentum within the entrained region of interest, and (c) steam condensation and characterization of droplets. These key physics phenomena are discussed in detail below, as well as the POI impacts on figures of merit (FOM) used to determine accident safety criteria acceptance.

### *2.1. Two-Phase Flow Regimes*

Two-phase flow typically means the interaction of two phases of matter in a fluid flow. In LWRs, there would be liquid water and steam. Two-phase flows contain many complicated and high-uncertainty phenomena that make them difficult to characterize and fully understand without rigorous instrumentation. Some of the complicating factors might include extreme differences in density and buoyancy, compressibility, liquid surface tension, phase velocities, direct contact condensation, and viscosity differences. The interaction of these phenomena, as well as others not listed here, cause the flow to have wildly different appearances, but that can be categorized based on the direction the pipe is traveling in, the superficial velocities of the fluids, pipe diameter, liquid and gas physical properties, and volume fraction occupied by each phase. The discussion in this paper will be limited to fluid transport through a horizontal pipe, as that best represents the MSL exit of a steam generator Two-phase flow through a horizontal pipe can be classified as bubbly, stratified, stratified-wavy, plug, slug, annular, or mist flow [7]. The two-phase flow regime diagrams are visualized in Figure 2. The lowest void fractions and superficial gas velocities would be seen in bubbly flow. On the other end of the spectrum, annular flow results from high vapor velocities and void fractions, where the liquid is held against the wall of the pipe in a thin film and the vapor travels through the center core of the pipe. Liquid droplets may also break off this film and become entrained in the vapor. When vapor velocity is at its highest, mist flow can be the result for horizontal and vertical pipes, characterized by essentially all the liquid components of flow entrained as droplets in the vapor. This is not illustrated in the following figure but results at the highest superficial gas velocity where the surface tension of the liquid film is not high enough to maintain a continuous liquid phase.

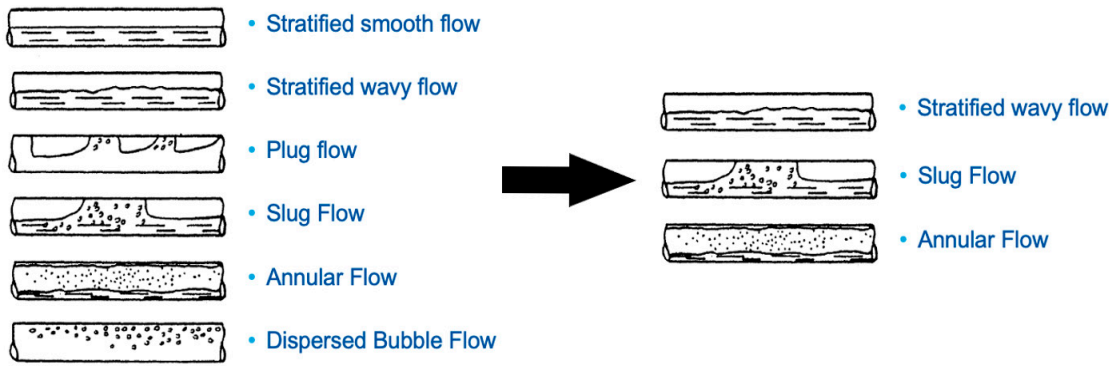


**Figure 2.** Horizontal two-phase concurrent flow regimes and the regimes downselected for applicability in a liquid entrainment study. Adapted from [8].

#### 2.1.1. Energy Being Moved by Addition of Liquid in Vapor

If vapor flow is entrained with liquid or is in some two-phase flow configuration, it will carry more energy by including the liquid than if it were just pure superheated vapor. Using water as an example to highlight this, at a pressure of 1 bar, water and steam can exist together in a saturated mixture at a temperature of 99.6 °C. The enthalpy of water and steam in these conditions is 417.51 kJ/kg and 2675.1 kJ/kg, respectively [9]. Per unit mass, steam holds a higher energy because it has absorbed the latent heat of vaporization

for its phase change, but this also results in a much lower density. Using the densities of the two phases, enthalpy can be converted to an energy density of 400.25 MJ/m$^3$ for water and 1.58 MJ/m$^3$ for steam [9], which is a difference of greater than 250 times. At the upper end of possible nuclear system pressure, this gap does narrow but there is still a significant contrast in energy density. Highlighting these differences shows that liquid entrainment in steam during an accident scenario could be beneficial to removing energy from the core if there is sufficient water inventory available to replace it.

#### 2.1.2. Mechanism of Droplet Formation and Size Distribution

Several visualization experiments were conducted that provide insight into the mechanism of droplet entrainment. Entrainment takes form due to several named mechanisms. The first is called bag break-up and is characterized by a small disturbance wave being blown up into a structure resembling a bag and stretching until the thin film is ripped apart, creating tiny droplets with an average radius of 100 µm [10]. The rim then breaks apart into much larger drops, on the order of 1 mm average radii [10]. The experiment focuses on sea-spray production due to high-wind estimates that the bag break-up mechanism produces about one hundred droplets per event [10]. The ligament mechanism was found to occur on all types of film instabilities and simultaneously with the bag break-up mechanism [11]. This will appear as the crest of an instability wave being elongated by the vapor flow until it is broken into several droplets, far fewer than with a bag break-up. Some of these will return to the liquid, while others may be broken apart further to remain entrained with the vapor [12]. Droplets resulting from the ligament mechanism can also be projected on the upper side of the pipe and help form the upper film of annular flow [11]. The last mechanism of entrainment is the result of previously entrained droplets striking the liquid film and knocking additional droplets into the vapor flow [13]. This is known as droplet impingement and only occurs after some other mechanism has created the droplets to become de-entrained. The incidence of droplets rejoining the continuous liquid phase is called deposition and occurs constantly if this continuous liquid phase is present. The difference in rate between entrainment and deposition should be considered as net entrainment.

### *2.2. Related POI and FOMs*

The purpose of improving the SOK is to have a more accurate accident analysis when low-SOK phenomena may have a significant effect. In the examples used here, the MSLB and SGTR, the effects of entrainment are propagated throughout the system and greatly impact the FOMs, which must remain within the design basis of the NPP. For instance, entrainment from the steam generator will cause a more significant accident progression during both aforementioned examples. This challenges the core's coolability, which is measured by cladding and fuel temperatures, as well as the margin to the minimum departure from nucleate boiling ratio (Equation (3)), risking dryout of the fuel rods. The MSLB poses an especially significant challenge to containment pressure and temperature limits. When entrainment is present, the liquid flashing inside the containment would accelerate the pressure rise, as well as increase the rate at which the steam system depressurizes, further challenging the containment pressure mitigation strategies. There are more examples of the permeation of entrainment to other phenomena relevant to design-based accident scenarios, and the fact that entrainment has a low SOK for SMRs creates urgency in the need for experimental and M&S investigations.

$$MDNBR = \frac{q_{chf}}{q_{local}(z)} \tag{3}$$

where

$q_{chf}(x)$ = critical heat flux
$q_{local}(x)$ = local heat flux during operation

## 3. Experimental and Modeling Approaches

Experimentation, as well as M&S, play key roles in investigating physics phenomena focused POI, which are important to safety evaluations. However, an optimal solution could be achieved by leveraging learning from experiments and M&S in tandem. Early-stage M&S accelerates the experimental design and testing plans; later, experimental data are required to verify and validate (V&V) the M&S tools, methods, models, and results. This section describes previous studies and approaches in both experiments and M&S, as well as how they can improve the applicability and knowledge gained from each other.

### *3.1. SET and IET: Significance, Difference, and Applications*

NPP system experimental testing is of paramount importance in designing and certifying nuclear reactor designs. M&S of physical systems must be consistently informed and supplemented with investigations of the phenomena in the physical world. Empirical testing of nuclear systems can be broken down into two main categories: separate effect test (SET) and IET. As the names may suggest, SETs will narrow the scope to a smaller number of phenomena with the purpose of capturing more detailed information on what is deemed as the most important. IETs, on the other hand, will focus on the integration of whole systems to gather information on their interplay and whole-system behavior on a smaller physical scale. For nuclear applications, both types of testing facilities are needed for licensing purposes if new concepts, components, or component combinations are being applied in a new reactor design. Both facilities can also be used to inform the design process and validation activities and are not necessarily only for passing through the licensing process. For this proposed investigation, a representative IET will have entrainment throughout the system, impacting the performance of many components. However, an SET of the steam generator with a focus on the steam generator outlet to MSL inlet, and an SET of containment to model the effect of entrained liquid flashing, would provide greater knowledge gain for this POI than the IET can alone, as SETs can better isolate specific phenomena.

### *3.2. Reviewing Previous Experimental Programs*

A large proportion of previous droplet entrainment experiments were performed with non-condensable gas (NCG), like air, to simulate some of the effects of boiling to produce liquid entrainment. The best comparison between air bubbles and steam bubbles in a pool boiling entrainment investigation comes due to bubble bursting on the surface. This produces small droplets that the air flow may entrain and carry out of the vessel. Using air, however, neglects the effect of heat transfer between the phases. An NCG phase with water can produce two-phase flow regimes with applicability to steam investigations. These may best be utilized in targeted SET investigation of fundamental entrainment phenomena, such as the mechanisms of entrainment initiation and deposition.

The first of the air–water investigations comes from [14], who experimentally investigated droplet entrainment from pool boiling at prototypic gas flux for an AP1000 during a small break loss of coolant accident (LOCA). The aim of this testing was to fill in a literature gap relative to higher gas flux to show applicability of an entrainment rate correlation proposed by [6] based on the two-phase mixture height and superficial gas velocity, which they found good agreement with. The researchers acknowledged that their pool height measurement method of using an averaged guided wave radar was not representative of the significant fluctuations. A year later, ref. [15] performed similar tests in the momentum-controlled region of the Kataoka correlation with both top and side exits for the gas/entrainment. The author's earlier model and the previously mentioned correlation overpredict entrainment for the side exit at a high-gas flux, so a new correlation was developed to address this. They performed a CFD calculation with a side exit and hypothesized that only entrainment produced near the region of high velocity by the exit will be carried out of the vessel [15]. Ref. [16] performed steam/water tests at the APEX-1000 test facility to study entrainment through the ADS-4 (Automatic Depressurization System) valves of

the AP1000 during depressurization. These tests indicated that entrainment was impacted largely by the water level's proximity to the hot leg. Ref. [17] shows that the ADS-4 has two separators for the steam/water mixture and two different sized steam pipes for the outlet of these to allow just single-phase liquid through the liquid exit. The liquid lines are recombined and piped into the primary sump, which has load cell transducers to measure its weight. Steam/water tests on ADS-4 entrainment at the Automatic Depressurization and Entrainment Test Loop (ADETEL) facility were performed by [18], which utilized a weighing tank to separate and measure the entrained liquid. The results of their testing also indicate that entrainment is driven by the water level in the reactor pressure vessel (RPV). In addition, these tests were run with and without reactor vessel internals installed, showing that increasing flow speed due to reduced gas space has the effect of increasing overall entrainment amount. Ref. [2] performed droplet entrainment experiments in a horizontal pipe with stratified air/water flow, measuring the droplet parameters with stretched conical single optical fiber probes. Varying the gas and liquid superficial velocities provides an increase to the overall liquid entrainment, but only an increase to the gas velocity decreased the mean droplet size. The REGARD facility, described by [19], is a SET facility designed to simulate two-phase flow in a PWR hot leg during the reflood process. Using air and water in a stratified flow, instruments were installed to gather information on droplet velocity, size, and mass flux of droplets and air, as well as water layer depth, wave frequency, and height. This researcher developed a new mechanistic model for entrainment in wavy stratified flow through a large diameter pipe at atmospheric pressure conditions. Finally, ref. [20] developed three correlations for droplet entrainment from a pool based on several empirical datasets. The authors claim these correlations are relevant to a wide range of thermal conditions, pressure, vessel and pool size, flow regimes, and superficial gas velocities up to 5.0 m/s.

The nondimensional equations of Table 1 are represented in the following equations. Equation (4) is the dimensionless superficial gas velocity, Equation (5) is the dimensionless height above the pool, and Equation (6) represents the dimensionless hydraulic diameter.

$$j_g^* = \frac{j_g}{\left(\frac{\sigma g \Delta\rho}{\rho_g^2}\right)^{\frac{1}{4}}} \tag{4}$$

where

$\rho$ = surface tension
$g$ = acceleration due to gravity

$$h^* = \frac{h}{\sqrt{\frac{\sigma}{g\Delta\rho}}} \tag{5}$$

$$D_H^* = \frac{D_H}{\sqrt{\frac{\sigma}{g\Delta\rho}}} \tag{6}$$

where

$D_H$ = hydraulic diameter

**Table 1.** Entrainment correlations developed from empirical study.

| Study | Correlation | Applicability | What Correlation is for | Uncertainty |
|---|---|---|---|---|
| [6] | i. $E_{fg}(h, j_g) = 4.84(10^{-3})(\frac{\rho_g}{\Delta\rho})^{-1.0}$<br>ii. $E_{fg}(h, j_g) = 5.417(10^{6}) j_g^{*3} h^{*-3} N_{\mu g}^{1.5} D_H^{*1.25} (\frac{\rho_g}{\Delta\rho})^{-0.31}$<br>iii. $E_{fg}(h, j_g) = 7.13(10^{-4}) j_g^{*3} N_{\mu g}^{0.5} (\frac{\rho_g}{\Delta\rho})^{-1.0} e^{-0.205 \frac{h}{D_H}}$<br>where $E_{fg}$(h,$j_g$) is the entrainment amount at height h above the pool and gas velocity $j_g$, $\rho_g$ is the gas density, $\Delta\rho$ is the density difference between liquid and gas, $j_g^*$ is the dimensionless superficial gas velocity, $h^*$ is the dimensionless height above the pool surface, $N_{\mu g}$ is the gas viscosity number, and $D_H^*$ is the dimensionless hydraulic diameter | i. Near pool surface<br>ii. Intermediate/ momentum-controlled region<br>iii. Deposition-controlled region | Air/water and steam/water pool entrainment | Not provided |
| [15] | $E_{fg} = 1.0(10^{25}) \left( \frac{j_g^*}{h^*} \right)^{10.05}$ | High gas flux region: $\frac{j_g^*}{h^*} \geq 3.34(10^{-3})$ | Air/water pool entrainment into pipe through upper plenum side exit | Not provided |
| [2] | $S_E = 9.18(10^{-6}) \frac{\mu_l}{D} We_g^{2.107} Re_l^{0.7} (D^*)^{-1.652}$<br>where $S_E$ is the droplet entrainment mass flux, $\mu_l$ is the dynamic viscosity of the liquid, D is the inner pipe diameter, $We_g$ is the Weber number of the gas, $Re_l$ is the Reynolds number of the liquid, and $D^*$ is the dimensionless pipe diameter | $65{,}500 \leq Re_g \leq 571{,}400$<br>$170 \leq Re_l \leq 11{,}000$ | Air/water entrainment and de-entrainment in a horizontal pipe section | Mean absolute percentage error of 14.3% |
| [19] | $\Gamma_E = \frac{\rho_l V_E}{\lambda_c^2 \tau_C}$<br>where $\Gamma_E$ is the entrainment rate, $\rho_l$ is the density of the liquid, $V_E$ is a sub correlation for the entrained volume, $\lambda_c$ is a sub correlation for critical wavelength, $\tau_C$ is the sub correlation for characteristic time | Only valid for horizontal stratified flow. Entrainment only from wave fragmentation, no other sources considered. | Air/water entrainment in horizontal pipe flow | Six probes in vertical array, each with droplet mass flow rate uncertainty of 0.003 g/s |
| [20] | $E_{fg} = \begin{cases} \gamma_1 e^{\gamma_2 \frac{j_g^*}{h^*}} & 0 \leq j_g \leq 0.05 \text{ m/s} \\ \gamma_3 \left( \frac{j_g^*}{h^*} \right) + \gamma_4 & 0.05 \text{ m} \leq j_g \leq 0.1 \text{ m/s} \\ \gamma_5^* \left( \frac{j_g^*}{h^*} \right)^{\gamma_6} & j_g > 0.1 \text{ m/s} \end{cases}$<br>where $\gamma_x$ are constants, $j_g$ is the superficial gas velocity | • Pressure = 1–15 bar<br>• Pool diameter = 0.19–3.2 m<br>• $j_g \leq 5.0$ m/s | Droplet entrainment from pool from bubbly to churn turbulent flow | $2 \times 0^{-5}$–$5 \times 10^{-5}$ for bubbly and transition flow regimes |
| [21] | $\frac{\left(\frac{E}{E_M}\right)}{1-\left(\frac{E}{E_M}\right)} = \frac{A_2 \left( D U_G^3 \rho_L^{\frac{1}{2}} \rho_G^{\frac{1}{2}} \right)}{\sigma \mu_T}$<br>where E is the entrained liquid fraction, $E_M$ is the maximum entrainment, $U_G$ is the gas velocity, $\rho_L$ is the liquid density, $\rho_G$ is the gas density, $\sigma$ is the surface tension, and $\mu_T$ is the terminal velocity | iv. $2.31 \text{ cm} \leq D \leq 9.53 \text{ cm}$<br>v. $11 \text{ m/s} \leq U_G \leq 131 \text{ m/s}$<br>$1.26 \leq \rho_G \text{ [kg/m}^3\text{]} \leq 2.75$ | Air/water entrainment and deposition in a horizontal cylindrical pipe | Not provided |

Reviewing some of the experimental correlations presented reveals a commonly identified nondimensional relationship indicating a potentially strong influence on the measured entrainment. This is the ratio of normalized superficial gas velocity to normalized height above the pool ($\frac{j^*}{h^*}$). This nondimensional group represents the tendency of droplets produced by a boiling pool to become entrained in the gas flow when the vapor velocity is higher, and the location of interest is closer to the pool surface. Several of the correlations presented in the literature indicate that entrainment may be exacerbated at the SMR-scale because the height of water during normal operation in the steam generator or RPV would be closer to the vessel exit than their large-scale analogue. The distance to vessel exit is closed even more rapidly in a depressurization or SGTR event. Experiments identify a strong dependence of entrainment amount on the distance droplets must travel to escape the vessel. This is because the significantly smaller flow area of the exit causes an increased gas velocity through the exit pipe. There is a strong relationship between gas velocity and the tendency to entrain droplets, therefore, closer proximity to this higher velocity zone will decrease the amount of entrained liquid that is deposited back into the pool.

Some very important IETs and SETs come from the Cylindrical Core Test Facility (CCTF) and Slab Core Test Facility (SCTF) in Japan and the Upper Plenum Test Facility (UPTF) in Germany [22]. These tests mainly focused on the reflood period following a core uncovery and overheating due to a large break LOCA, looking at entrainment in the

upper core and upper plenum, hot legs, and steam generators, as well as de-entrainment in the upper plenum, hot legs, and steam generator during emergency core cooling (ECC) injection. The CCTF and SCTF IETs were used for end-of-blowdown to refill to reflood tests with cold leg ECC injection tests. When the RPV was venting up the downcomer into containment during the blowdown, ECC was entrained with the steam and did not reach the core until the flow rate was low enough. Early in reflood, water was entrained with the steam produced at the bottom of the core, which could de-entrain in the upper plenum and become re-entrained or fall back to the core. The entrained liquid may also accumulate at the steam generator inlet and hot legs. After the accumulators stopped injection during reflood and the system switched to low pressure coolant injection, the CCTF saw vaporization and superheat of all the entrained water that reached the steam generators because the secondary side was hotter. A two-phase mixture exited the cold leg break during low pressure coolant injection. These facilities were instrumented with multiple points of differential pressure (DP) measurement throughout the core height that were effective in identifying entrainment because of the resulting pressure drop. The UPTF facility was capable of both IET and SET, which focused on entrainment in the downcomer during reflood with cold ECC injection and de-entrainment on the flow path from the core to the steam generators. One important finding at the UPTF SET, which had a larger scaled downcomer than the CCTF, is that the entrainment is larger out of the cold leg break. SET was also performed for de-entrainment where upon water injection to the UPTF core simulator, de-entrainment accumulation was found to have started first in the upper plenum, then in the steam generator inlet plenum, and finally in the hot legs. Carryover into the steam generator tubes happened eventually with enough accumulation. The Integral Test Facility Karlstein (INKA) was developed for testing of the AREVA BWR, KERENA [23]. This was designed for IET and SET of many of the passive safety systems of the KERENA reactor design, including the performance of its pressure suppression containment in the case of a LOCA and coolant release to containment. Table 2 summarizes previous experimental approaches to entrainment analysis.

**Table 2.** Relevant droplet entrainment experimental programs.

| Facility | SET or IET | Gas | Relevant Measured Parameters | Instruments Used: Measurement Uncertainty | Significant Findings |
|---|---|---|---|---|---|
| AP1000 Upper Plenum/Hot Leg Entrainment Facility [14,15] | SET | Air | i. Entrainment amount<br>ii. Pool level (time-averaged)<br>iii. Air-flow rate | i. Load cells: ±2%, sampling paper: ±5%<br>ii. Visualization system and Guided Wave Radar: ±10 mm<br>iii. Vortex flow meters: ±0.5% each | Investigated entrainment correlation differences for top and side vessel pipe exits |
| APEX-1000 [16] | IET | Steam | i. Entrainment amount<br>ii. Separated steam-flow rate<br>iii. RPV water level | i. Load cells: NP<br>ii. Vortex flow meters: NP<br>iii. Differential pressure (DP): NP | Entrainment amount driven by pool surface proximity to hot leg |
| ADETEL [18] | SET | Steam | i. Entrainment amount<br>ii. RPV mixture liquid level<br>iii. RPV collapsed liquid level<br>iv. Weighing tank steam exit flow rate | i. Weighing transducers: ±0.02%<br>ii. Capacitance probe: ±0.2%<br>iii. DP transducers: ±0.02%<br>iv. V-cone DP flow meter: ±1.5%, could be higher | RPV vessel internals increase net entrainment from increased vapor speed |
| Pusan National University—Horizontal Stratified-Wavy Entrainment Testbed [2] | SET | Air | i. Air mass flux<br>ii. Water mass flux<br>iii. Droplet velocity<br>iv. Droplet diameter<br>v. Droplet mass flow rate | i. Thermal mass flow meter: ±0.78 kg/m$^2$s<br>ii. Coriolis flow meter: ±1.99 kg/m$^2$s<br>iii. Laser doppler anemometry (LDA): ±0.07%<br>iv. stretched conical single optical fiber probes: ±9%<br>v. stretched conical single optical fiber probes and LDA: NP | Increasing gas and liquid superficial velocities both increase entrainment amount |

**Table 2.** *Cont.*

| Facility | SET or IET | Gas | Relevant Measured Parameters | Instruments Used: Measurement Uncertainty | Significant Findings |
|---|---|---|---|---|---|
| REGARD [19] | SET | Air | i. Air flow rate<br>ii. Water flow rate<br>iii. Droplet velocity and diameter<br>iv. Local droplet mass flow rate | i. Flow meter: <±2%<br>ii. Flow meter: ±5%<br>iii. Laser particle analyzer: variable, NP<br>iv. Isokinetic probe: ±0.003 g/s | Developed mechanistic model for entrainment in large-diameter pipe |
| CCTF [22] | IET | Steam | i. Steam break flow rate<br>ii. Water break flow rate<br>iii. Void fraction<br>iv. Liquid level | i. NP: NP<br>ii. NP: NP<br>iii. Impedance probes, gamma densitometer: NP<br>iv. Conductivity and optical liquid level detectors (LLDs): NP | During reflood, entrained water would vaporize upon reaching the steam generator |
| SCTF [22] | IET | Steam | i. Hot leg entrainment amount<br>ii. Void fraction<br>iii. Liquid level | i. NP: NP<br>ii. Impedance probes, gamma densitometer: NP<br>iii. Conductivity LLD: NP | Entrainment during refill investigating different coolant injection locations |
| UPTF [22] | SET | Steam | i. Void fraction<br>ii. Liquid level | i. Gamma densitometer: NP<br>ii. Conductivity and optical LLDs: NP | Entrainment in downcomer during reflood was larger in the cold leg |
| INKA [23] | IET and SET | Steam | i. Void fraction<br>ii. Water level<br>iii. Drywell gas composition<br>iv. Drywell pressure sensor | i. Gamma densitometer: NP<br>ii. Thermo needle probes, DP: NP<br>iii. Mass spectrometer: NP<br>iv. NP: NP | Test findings not presented |

NP = Not provided by the authors.

Experiments have exposed entrainment's heavy dependence on the flow direction of both phases. When they travel in the same direction, such as leaving the steam generator and traveling through the MSL, this is concurrent flow. Entrainment can happen to a large degree, but this requires high superficial velocity. Concurrent flow can be compared with countercurrent flow to elucidate the impact. The downcomer of an RPV will often experience full entrainment of the liquid when the system is attempting to recover the core. This is because the liquid is attempting to fall with gravity and the steam produced in the RPV tends to move in the opposite direction, which is called countercurrent. The two-phase flow phenomenon of full flow reversal of the liquid is called the countercurrent flow limitation.

The previous decades of experimental work on droplet entrainment have developed the body of knowledge extensively. These works have produced several impactful findings, such as empirical relations between water level, vapor flow direction, and fluid flow velocity on the rate of entrainment. In addition to this, entrainment behavior during nuclear core uncovery scenarios, including the impact of entrainment on accident progression and recovery, has also been documented. These are most valuable for the existing large-scale NPP systems they are scaled for, but experiment design lessons can be applied to future experimental programs. With previous approaches utilizing either steam or air as the gas phase, a future experiment design should include an NCG fraction with the steam flow. This would be present in nuclear accidents as they precipitate out of solution or are injected by a component such as an accumulator. NCGs would harm heat transfer between coolant phases and could have significant impact on entrainment development. Another significant gap identified in the literature is how coolant and entrainment impact core uncovery and reflood for an RPV designed for coolant piping penetrations only above the elevation of the fuel. This has the greatest impact during the aforementioned accident phases and should have representative experiments for the next generation of SMR.

### *3.3. Measurement and Instrumentation*

Table 3 summarizes the parameters to measure, as well as the instrumentation options. The table includes a brief discussion on operating principles of each instrument, as well as how they may apply to an entrainment study. Precise measurement of critical parameters is crucial to constructing an entrainment model useful in accident modeling and analy-

sis. Uncertainty is inherent to experimentation, but careful selection of instrumentation can limit the compounding uncertainty of a calculated parameter built on fundamental measurements [24].

**Table 3.** Parameters to measure and instrumentation options.

| Measurement Parameters and Instrumentation Options | | Working Principles | Engineering Application for SMR Systems and Applicability to Entrainment Study |
|---|---|---|---|
| Void Fraction | Wire-mesh sensors (WMS) [25] | Capacitance or conductance between cells interpreted as a void fraction: $\alpha_{i,j,k} = 1 - \frac{\sigma^{meas}_{i,j,k}}{\sigma^{lo}_{i,j}}$ where α for void fraction; σ for conductance (for the measurement liquid phases only); i, j, k are the mesh indices for row, column, and frame; *meas* is the measured conductance; and *lo* is the calibrated conductance for liquid only | • Can only be used effectively in a pipe cross section<br>• Good assessment of flow regime and average void fraction. |
| | Radiative [26] | Radiation is attenuated more traveling through liquid, average void fraction over time: $\alpha = \frac{\ln(I) - \ln(I_L)}{\ln(I_G) - \ln(I_L)}$ where I for radiation intensity measured by the receiver, $I_L$ for intensity when pipe filled with water, $I_G$ for intensity when pipe filled with gas. | • Suitable only for small-diameter pipes or high void fraction<br>• Flow must be well mixed<br>• Low applicability to proposed entrainment study. |
| | Ultrasound [27] | Real-time measurement with sensors picking up reflected sound waves across pipe: $\delta = c\left(\frac{t_\delta}{2}\right)$ where δ for film thickness, c for speed of sound in liquid at reference temperature, $t_\delta$ for time difference between interfaces. | • Best used for low void fractions<br>• Low applicability to this study because of the wide range of expected entrainment amount. |
| | Impedance | Localized point measurements based on same principles and equation as the WMS. | • Fast and cheap method of point or average measures if made into an array of probes<br>• Could be used in the steam generator or containment vessels in the entrainment study. |
| | Visual [28] | Optical fiber probes utilize principle of internal reflection to determine the phase of fluid: $1 > \frac{n_1}{n_2} \cdot 0.7071$, for 45°-chamfered tip where $n_1$ for refractive index of optic material, $n_2$ for refractive index of fluid. | • Fast and cheap point measurements<br>• Could be used anywhere, especially in the steam generator or containment for the entrainment study. |
| | Separating liquid from vapor | Uses moisture separators and measurement of single phases to estimate pre-separation void fraction. Can measure either vapor or liquid flow rate, or measure mass change of liquid holding tank for an average entrainment over time | • Important to correctly choose separator type and account for energy loss in separator<br>• Could be applied to steam generator SET. |
| | Quick-closing valve technique | Isolating pipe section with simultaneous valves to measure liquid fraction. Some inherent inaccuracy due to disruption of flow during valve closure. | • Disruptive to testing, requiring a restart of system after measurement.<br>• Severe testing disruption is undesirable for entrainment study. |
| Superficial Phase Velocities | Three-layer WMS | Bubble tracking algorithm can interpret gas phase velocity in pipe during bubbly flow. | • Likely not useful for droplet entrainment because of liquid holdup in sensor. |
| | Pitot tube [29] | Employs Bernoulli's principle of pressure change with velocity: $v = \sqrt{\frac{2(p_t - p_s)}{\rho}}$, for fluid velocity where $p_t$ for the total pressure, $p_s$ for the static pressure, ρ for the density. | • Measurement can be disrupted by multiple phases if not in stratified flow<br>• Likely low applicability for this entrainment study. |
| Temperature | Thermocouple (TC) [30] | Temperature induces voltage between two different metals at tip of TC: $T_{Hot} = \frac{E_{emf}}{S} - T_{Cold}$ where $T_{Hot}$ for the temperature being measured, $E_{emf}$ for the voltage output of the $T_C$, S for the Seebeck coefficient, $T_{Cold}$ for the cold-junction temperature | • Accuracy under wide range of temperature and pressure conditions<br>• Requires more frequent calibration<br>• May be used in entrainment study for their low cost. |
| | Resistance temperature device [31] | Temperature change induces linear change in resistance: $R = R_0(1 + \alpha_T \Delta T)$ where $R_0$ for the resistance at 0 °C, $\alpha_T$ for the temperature coefficient of resistance, ΔT for the temperature change. | • More expensive, slower response, but higher accuracy and stability<br>• Preferred method in areas not requiring transient analysis. |
| | Fiber optic sensors | Cables take discrete temperature measurements every 1 mm–1 cm and provide live monitoring. Output usually converted to temperature by accompanying device. | • Durable and non-intrusive<br>• Potential for steam generator and containment SET facility monitoring. |

**Table 3.** *Cont.*

| Measurement Parameters and Instrumentation Options | | Working Principles | Engineering Application for SMR Systems and Applicability to Entrainment Study |
|---|---|---|---|
| Flow Rate | Coriolis flowmeter [32] | Induces vibration in a tube to measure angular momentum produced by Coriolis effect of the flowing fluid: $mass\ flow = \frac{F_C}{2wx}$ where $F_C$ for the Coriolis force, w for the angular velocity, x for the tube length. | • Very accurate measurement of gas or liquid in single-phase<br>• Good option for measurements after separating phases. |
| | Vortex flowmeter [33] | Bluff body creates vortices in the fluid, with the frequency proportional to the fluid velocity: $V = \frac{fd}{St}$, for fluid velocity where f for the vortex shedding frequency, d for the bluff body width, St for the Strouhal number. | • Best used for single-phase gas or liquid with higher velocities<br>• Good candidate for the entrainment study if new equipment is needed and cost is a concern. |
| Liquid Level | Float gauge | Designed to follow the surface of the liquid in a tank, can output signal to a data acquisition system or be a visual gauge. Will be partially submerged depending on specific gravity of it and the liquid. | • May not be dependable in a violently boiling region<br>• Could provide visual indicator as backup to other methods. |
| | DP [34] | Difference in pressure between the bottom and top of the vessel infers liquid level: $H = \frac{DP}{SG}$, for height of the liquid where SG for the specific gravity of the liquid. | • Can provide average liquid level even while boiling<br>• Proven and dependable method to be used in the entrainment study. |
| | Ultrasonic or Radar sensor [35] | Bounces sound or light waves off surface of liquid with delay determining distance: $D = \frac{cf}{2}$, for distance from sensor where t for time between transmission and detection. | • Accurate average level measure when liquid is too corrosive for contact methods<br>• Can be used effectively for entrainment study. |

#### 3.3.1. Instrument Placement Impact on Measurement

Void fraction measurements can be heavily skewed by the instrument used, especially in an entrainment study, therefore, it is best if wire-mesh sensors are avoided for entrainment measuring. This is due to the intrusiveness of the mesh on the flow where the instrument acts as a sudden expansion and contraction, thus changing the flow characteristics [25]. Point measurements or non-contact methods, like radiative or ultrasound, are good options if consideration is given to when they may not provide accurate results. Ref. [36] makes the point that non-heterogeneity in flow phenomena decreases the sensitivity of ultrasound void fraction measurements. A similar principle would also apply to radiative means due to the nature of single transmission and receiver systems. There is an inherent inaccuracy that would come with attempts at void fraction measurement in pipe flow until the flow has reached a well-developed stage. In a steam generator partially filled with boiling liquid, or containment where the wall will form a condensate film, the location of temperature or void fraction sensors could be either totally submerged in liquid film or measure a two-phase mixture, dependent on distance to the surface and testing conditions. The distribution of these sensors is important to collect a variety of two-phase and single-phase information. However, these sensors cannot become too numerous so as to influence the behavior of the system. It may be more desirable to have a single fiber optic cable for temperature measurement stretching the length of the steam generator tubes than it would be to place an array of TCs. Any instrument in a two-phase region will also be a point of de-entrainment for droplets; those entrainment data could be skewed if this effect is made too significant by aggressive instrumentation.

#### 3.3.2. How Experiments and Computational Models Improve Each Other

The only way to improve computational models is by comparison to experimental results and adapting the correlations used in the model to improve modeling accuracy in the process of validation. Experimental instrumentation is coarse to inform CFD more generally so the CFD model can be used for insight into complex physics phenomena not captured by instrumentation. CFD simulations can be performed more quickly and cheaper than the experiments, so these can be used to narrow the scope of the experimental program. The Reactor Excursion and Leak Analysis Program (RELAP) is a system-level

code that can set the initial and boundary conditions for each of the accident scenarios that would be applicable. An optimum range of testing variables can be found by using computer modeling to identify the most impactful conditions. Additionally, preliminary CFD analysis can help to identify the key parameters affecting safety results and guide the selection and placement of instrumentation. Finally, the process described in this subsection is iterative, where empirical data are constantly used to improve the CFD models, which can then be used to refine experiment design. CFD excels in component or sub-component investigation as the results are highly detailed and the M&S scope must be limited for computational cost reasons. As such, it is best used to supplement an SET where detailed validation data are available. In both an IET and SET, however, it can be used to provide local insight into the physics phenomena at a smaller scale than instrumentation is likely to capture. On the other hand, RELAP will excel at full-system analysis comparable to the IET, as well as the bulk behavior of larger components like the steam generator.

Several challenges are presented in pursuit of model validation. First among these is the resource constraint of a robust experimental program combined with a hybrid effort of model development. Experiments can cost significant sums in both time and money to construct and operate so the focus is often limited to only the necessary components and scenarios, which can be difficult to identify. Model development often requires less capital expense but does not come with reduced time requirements. Another significant challenge in this effort is the pitfall of overfitting the model. As a model is made more complex to reflect the experiment design and is tuned once empirical results start being produced, there is a risk of overcorrection for the model parameters. The result of this would be a narrowing of the scope that this model can be applied to, creating a model that may mirror the results of the scaled facility but that is not representative of a larger-scale prototype facility the model was created in pursuit of. A proper model development process will balance complexity and simplicity to capture important physics phenomena without falling into overfitting based on the experimental data.

### *3.4. CFD Modeling Approaches*

A method of analyzing expected entrainment in a system under a given set of conditions involves utilizing CFD, which is an area of study that leverages computing power to approximate the solutions to the five coupled Navier–Stokes equations for fluid flow [37]. Generally, CFD approaches can be split into two categories, Lagrangian and Eulerian, but can also take a hybrid approach. The Lagrangian approach follows a fluid element moving as one unit through a flow without interaction between the elements [38]. The smooth particle hydrodynamics method within the Lagrangian approach defines a finite volume for each element, which can overlap multiple grid cells for smooth calculations of particle movement [38]. Ref. [39] applied smooth particle hydrodynamics in the creation of an airblast atomizer and found the method to be advantageous over Eulerian approaches due to the continuous tracking of particles and reduction in computational effort for many individual particles. A strict Eulerian approach for two-phase flow modeled air–water flow in a cyclone separator, interpreting each as Eulerian volumes that can exist in the same space with different properties [40]. Using ANSYS FLUENT with a Reynolds stress turbulence model, the results showed good agreement on the basic flow patterns in the pipe separator, but diverged with empirical data on specific quantities, while also being relatively computationally unstable [40]. Another such Eulerian–Eulerian model was used to analyze the entrainment through the T-junction of an AP1000 automatic depressurization system using the volume of fluid (VOF) approach and standard $\kappa$-$\varepsilon$ turbulence model [41]. Validating the computation with empirical data from the ADETEL facility, the CFD model showed good agreement on the effects of T-junction diameter ratio, horizontal pipe water level, and gas flow [41]. A combination approach can also be taken, as in [42]. This work utilized the Eulerian VOF approach to model an annular film flow with a gas core while converting detached droplets into a Lagrangian point particle (LPP). This approach, graphically represented in Figure 3, allows coarsening of the mesh around the LPP and reduces

computational effort, while showing similar prediction in entrainment behavior compared with a purely Eulerian VOF approach [42]. Finally, a hybridization effort was taken to predict the behavior of steel slag entrainment in argon gas upwelling during the steel refining process. The model takes a VOF approach for the liquid phases and discreetly tracks the bubble phase in a Lagrangian fashion using the large eddy simulation (LES) to resolve large turbulence structures [43]. The model does well to accurately predict bubble transport and size distribution, as well as the slag layer fluctuation, and slag droplet generation [43]. The final Eulerian–Lagrangian approach discussed modeled droplet entrainment from a sneeze to estimate contamination in a large indoor facility [44]. This work modeled a wide range of saline droplet sizes injected into the air during a finite event, along with the subsequent entrainment and de-entrainment during a transient simulation. These CFD investigations are presented in summary form in Table 4.

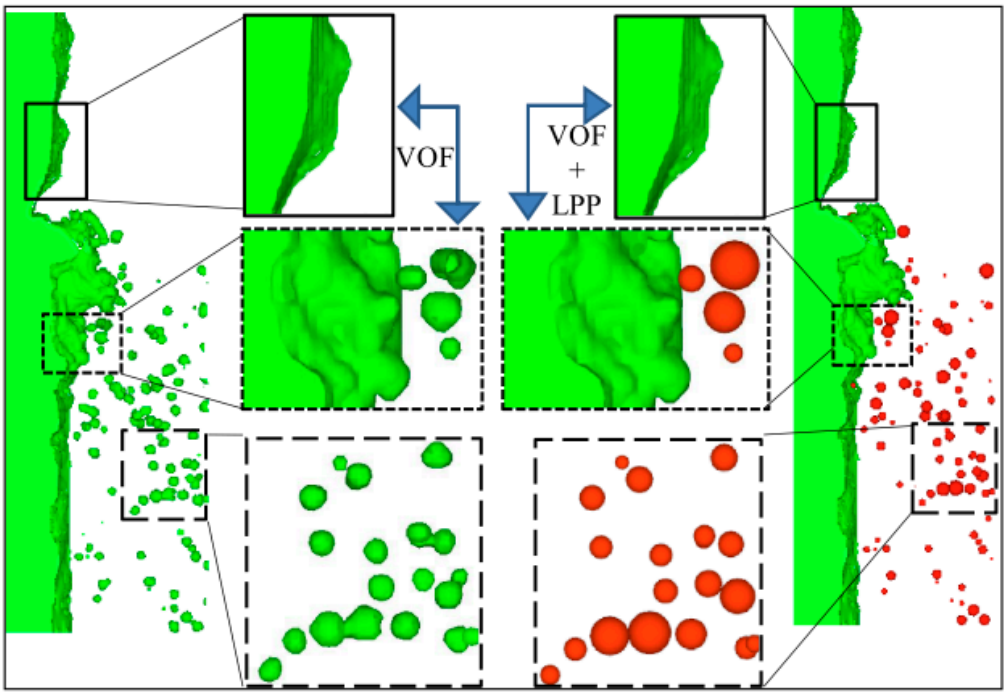


**Figure 3.** Application of the hybrid approach, modeling the continuous phases using the Eulerian VOF and the detached droplets using the LPP method. The red color in the right side of the figure indicates a differing modeling approach for droplets in the hybrid approach. Reproduced with permission from [42]. Copyright IOP Publishing, 2021.

The approaches discussed have strengths and weaknesses, especially considering their application. Of the methods described a hybrid approach of a Eulerian VOF combined with Lagrangian point particles could strike the right balance between accuracy and resource constraints. This reduces computational effort without a notable decrease in predictive capacity for entrainment. A downside to implementing this approach would be additional complexity in developing the model and setting up the simulation. The creation of models for droplet entrainment and two-phase flow involves many challenges. The first is that the governing Navier–Stokes equations are complex, making accurate modeling difficult and computationally expensive to attempt. Multi-phase interactions are also complicated and can be very difficult to measure, as instruments can tend to disrupt intricate flow patterns. This makes validation with experimental data harder, especially as fluid conditions approach more severe pressure, temperature, or corrosion conditions, exponentially increasing the cost of building experiments and decreasing the ability to implement sufficient instrumentation for CFD validation.

**Table 4.** Summary of entrainment modeling using CFD.

| Study | Modeling Approach | Applicability Range | Validation Results | Gaps |
|---|---|---|---|---|
| [39] | Lagrangian smooth particle hydrodynamics | • Isothermal flow<br>• Pressure proportional to density | • Not provided | Only applicable to air/water. |
| [40] | Eulerian–Eulerian | • Air/water pipe separator | • Qualitative agreement on tangential but did not predict axial or radial velocity profiles | Not computationally stable and droplets do not interact with each other. |
| [41] | Eulerian–Eulerian | • T-junction diameter ratio of 0.43–0.71<br>• Inlet turbulence intensity for water: 0.3–1.5% and 1–10% for air | • Good agreement with ADETEL results for entrainment | Only applicable to air/water with no heat transfer. |
| [42] | Eulerian VOF—Lagrangian Point Particle | • Annular flow<br>• Liquid-to-gas velocity ratios of 7–40, momentum flux ratios of $0.4 \times 10^{-5}$–$13.3 \times 10^{-5}$ | • Not provided | Only compared with the results of a different CFD approach. |
| [43] | Eulerian VOF—Lagrangian LES | • Slag entrainment from Argon bubble upwelling | • Validated for predicting unsteady bubble–slag behavior | Focused primarily on liquid mixing and not droplet entrainment. |
| [44] | Eulerian–Lagrangian | • Droplet size of 1–1000 μm<br>• 2–34 °C temperature range of air and droplets | • Good agreement with empirical data from the literature | Applies to low-temperature gas and liquid phases |

With that said, CFD analysis can be an important piece of the evaluation model development and assessment process (EMDAP), which is required in the NRC licensing of new reactors in the process defined by Reg. Guide 1.203 (REGULATORY GUIDE 1.203, 2005). Evaluation models are used for assessing reactor systems, subsystems, and components during Chapter 15 transient and accident events. CFD models that have been validated with empirical data can be used for detailed assessment of specific phenomena, like entrainment, to satisfy the NRC requirements for evaluation modeling.

### *3.5. System-Level Code M&S Approach*

RELAP5 is commonly used for system-level accident analysis and commonly pairs with the IET experimental approach, since this also models the whole system. This contrasts with CFD, which provides greater detail on a smaller scale. In this sense, M&S with CFD more closely reflects SET experimental modeling, though RELAP may also be used at the component level for an evaluation model. In RELAP5-3D, a later iteration of RELAP5, entrainment is most significant in annular mist flow, characterized by a liquid film attached to the wall and a high-velocity vapor core carrying entrained droplets. The entrainment model in RELAP provides the liquid volume fraction near the wall for the closure of the momentum and heat transfer equations. The liquid volume fraction is calculated differently based on whether the flow regime is in the vertical or horizontal directions but has parameters to include fluid properties and flow characteristics, as well as coefficients and constants that can be altered. The latter aspect of the entrainment model within RELAP5-3D can be corrected based on empirical data and is an important part of how experiments improve and eventually validate the evaluation model. An example of this cooperation of experiment and M&S comes from AP1000 testing of entrainment into the hot leg from ADS-4 activation. Initially, with no special entrainment in RELAP5/MOD3.4, the standard two-fluid six-equation model estimated entrainment within the bounds of 30% compared with the experimental results [45]. Attempting to reduce this error, the researchers then implemented a complicated mechanistic model, increasing error significantly. Finally, implementing a simple steady-state liquid mass conservation produced a highly refined entrainment estimate within their RELAP model, fitting within a 5% error compared with the experiments [45]. This represents the strength of running a parallel effort of M&S with the experimental program. There is a much stronger likelihood of achieving model validation sufficient to pass through the EMDAP.

### *3.6. Identification of Specific POI Relevant*

The primary POI in this study is entrainment, but several additional phenomena can cause, be caused by, or influence liquid entrainment in a gas. Coupled with entrainment, de-entrainment is the process whereby liquid droplets leave the gas space to rejoin the liquid film or volume. Related to this, the superficial velocities of liquid and gas have a big effect on the net entrainment rate.

Superficial velocity: All other factors being equal, the higher the superficial velocity of the gas, the greater the rate of droplet entrainment. However, the superficial velocity of the liquid also tends to have a similar effect on entrainment. The increasing turbulence of higher superficial liquid velocities increases the rate of entrainment of droplets [46].

Flash boiling: Another phenomenon with application to entrainment is flash boiling, which can be both a cause and effect of entrainment. In the scenario of an MSLB, the decreasing pressure will result in an increase in the rate of boiling in that loop, directly increasing the amount of entrainment. In this scenario, when the entrained liquid is expelled through the break, it will flash to vapor because of the sudden drop in pressure causing it to be a superheated liquid temporarily. This will increase containment pressure greater than purely superheated steam leaving the break.

Pressure drop: The pressure drop phenomenon was identified when researchers recognized that vapor would lose energy from entraining and accelerating droplets [47]. A larger pressure drop from increased entrainment will mean a lower volumetric flow rate out a break during choked flow, making this a POI worth investigating.

## 4. Findings and Discussion

Findings emphasizing physics and testing approaches are as follows:

- The relationship between entrainment and de-entrainment has been extensively explored, showing that droplets impinging on a liquid surface are de-entrained but can create smaller droplets that are entrained.
- SET testing with non-condensable air has an important place in assessing the physics of entrainment—how droplets are formed and distributed in the gas phase of a horizontal pipe.
- The entrainment phenomenon is heavily dependent on the specific geometry, as shown by previous testing of the RPV top exit vs. side exit and the inclusion of vessel internals. The air testing of RPV exit geometries may also qualitatively inform the expected results of a steam system, but the inability to consider vapor condensation prevents a direct quantitative comparison.
- The experimental facilities discussed provide a significant body of knowledge for entrainment out of an RPV and the associated level drop when connective piping is ruptured.
- The testing approaches utilizing steam and water with elevated temperature and pressure conditions are particularly attractive for the ability of the gas phase to condense.
- The INKA tests were the only experiments the author could identify that analyzed the effect of a blowdown occurring inside containment and the associated pressure response. However, this is only representative of the AREVA BWR and lacks the effect of entrainment in the steam flow.

After discussion of the coverage of previous empirical approaches, the existing discrepancies in knowledge between theoretical models and experimental data are significant. The gaps in empirical data are as follows:

- Effect on net entrainment from an internal RPV structure representative of an SMR. Likewise, the effects of entrainment on reactor system depressurization through break and corresponding containment pressure increase due to flashing.
- Entrainment resulting from coolant line break of the vessel with penetrations only above the core.
- Impact of inclusion of NCGs on droplet entrainment.

Experimental entrainment testing is desperately needed to prepare for the licensing of next-generation SMR technology. This effort will involve multiple testing facilities, a plethora of instrumentation for controls and analysis, and extensive CFD modeling to aid the experimental and licensing approaches. These aspects are detailed in the requirements for the future entrainment study:

- IET facility of representative SMR system, along with SET facilities of a steam generator and containment. Facility and testing design necessary to model entrainment from depressurization during a large break LOCA and MSLB, as well as from the level swell after an SGTR.
- To measure entrainment in the IET or from the steam generator SET, the phases should be separated and measured separately. Transients can be analyzed with a liquid flow meter.
- Flow rate instrumentation for the calculation of superficial phase velocities will be used along with vessel level measurements for comparison with previous empirical entrainment correlations which relied heavily on these two parameters.
- Flow rates of pure steam can be taken with vortex flow meters, water can use a Coriolis flow meter, and air as an NCG can use either.
- Ultrasonic or radar can be used for average level measurement, with differential pressure (DP) used for collapsed liquid level and measurement diversity.
- Optical fiber or impedance point probes for void fraction can be utilized in the RPV of the IET and both SET facilities to monitor entrainment or saturated steam distribution.
- Local temperature probes should be type-K thermocouples for the wide measurement range, and fiber optic cables can be used for non-intrusive temperature distribution detection in any facility.

Filling the literature gaps and improving the SOK is an important step in preparing for the licensing of diverse water-cooled SMR designs. With more data widening the coverage of the experimental literature, evaluation models can be further developed and honed to improve regulatory confidence.

*Air and Steam Testing Comparison*

Determination of which gas should be used for two-phase experiments comes from several factors. The primary concern will be the phenomena of interest and whether these are impacted significantly by the heat transfer component of steam–water interaction.

Fluid type: Steam has different physical properties of air, which has many components including water vapor, and steam is representative of actuality, improving data relevance for high-temperature applications. An investigation of droplet entrainment on safety during accident scenarios will require simulation using the real phases. The use of steam, however, is more hazardous, costly, and complicated. Air testing can use cheaper materials and less stringent safety controls, as well as smaller test facilities.

Test conditions: The trade-off includes less representative test conditions, but lower temperatures more easily allow for visualization of the flow and two-phase interactions by utilizing clear tubing instead of a material like stainless steel. Visualization in air–water has enabled much of the previous research into the specific mechanisms of entrainment and de-entrainment.

Geometric consideration: Another consideration for test design is the orientation of the facility. If a specific reactor or reactor component is being investigated, the major design features should be consistent with the test facility. However, if fundamental entrainment physics is the focus, flow orientation will have a significant impact on results. This is due primarily to the flow regime variance between vertical and horizontal flow. Vertical pipes eliminate the ability of the two phases to stratify, a flow regime that could produce droplet entrainment in horizontal pipes. Additionally, in horizontal pipes, gravity is a major mechanism of de-entrainment, pulling droplets toward the liquid region. This does not have the same effect in vertical flow because gravity cannot separate the phases discretely at low superficial velocities.

## 5. Conclusions and Future Research Directions

This study collects the main droplet entrainment modeling efforts and experiments to identify gaps in empirical knowledge while also assessing measurement parameters and instrumentation options important to future research. The general findings up to this point include the different mechanisms of droplet entrainment and its potential impact in an accident scenario. While much of the research was specifically focused on accident analysis of existing large-scale plants, there is a lack of understanding of how entrainment will play a role in accident scenarios for the next generation of nuclear reactors. Entrainment impacts multiple aspects of reactor operation. The specific effects are as follows:

- Entrainment causes a quicker depletion of the coolant inventory, limiting its ability to fully absorb the latent heat of vaporization for efficient cooling.
- Entrainment is potentially detrimental to containment integrity due to the rapid pressure increase in entrained liquid flashing to vapor after exiting the break.
- Due to the compact design of the new SMR class of reactors, the impact of entrainment on pressure boundary rupture accidents is exacerbated.

A suggested future research direction for entrainment testing including IET and SET facilities for a PWR SMR design is as follows:

- A scaled IET facility to inform the parameters of a two-phase release into a containment SET facility with an additional steam generator SET facility outfitted to model an SGTR scenario.
- Superficial phase velocity, vessel level, pressure, and void fraction measurements will be used to assess the applicability of entrainment correlations to SMRs.
- A parallel effort of CFD and RELAP M&S to inform the experimental program. The experimental results/data will be fed back into the models for correlation improvement and uncertainty quantification.

**Author Contributions:** Conceptualization, P.K.B.; methodology, K.L.F. and P.K.B.; investigation, K.L.F.; resources, K.L.F. and P.K.B.; writing—original draft preparation, K.L.F.; writing—review and editing, P.K.B. and P.S.; supervision, P.K.B. and P.S.; project administration, P.S.; funding acquisition, P.S. All authors have read and agreed to the published version of the manuscript.

**Funding:** This research was funded by the United States (U.S.) Department of Energy (DOE) Advanced Reactor Demonstration Project (ARDP) program office grant number ARDP-20-23819. Funding Opportunity Number DE-FOA-0002271, Risk Reduction Pathway.

**Data Availability Statement:** No new data were created or analyzed in this study. Data sharing is not applicable to this article.

**Acknowledgments:** The authors would like to thank the U.S. DOE National Reactor Innovation Center ARDP office and the Thermal Fluid Systems Methods and Analysis Department at Idaho National Laboratory for their encouragement and support.

**Conflicts of Interest:** The authors declare no conflicts of interest.

**Disclaimer:** This information was prepared as an account of work sponsored by an agency of the U.S. government. Neither the U.S. government nor any agency thereof, nor any of their employees, makes any warranty, expressed or implied, or assumes legal liability or responsibility for the accuracy, completeness, or usefulness, of any information, apparatus, product, or process disclosed, or represents that its use would not infringe privately owned rights. References herein to any specific commercial product, process, or service by trade name, trademark, manufacturer, or otherwise, does not necessarily constitute or imply its endorsement, recommendation, or favoring of the U.S. government or any agency thereof. The views and opinions of authors expressed herein do not necessarily reflect those of the U.S. government or any agency thereof.

## Nomenclature

### Abbreviations

| | |
|---|---|
| ADETEL | Automatic Depressurization and Entrainment Test Loop |
| ADS | Automatic Depressurization System |
| ARDP | Advanced Reactor Demonstration Project |
| BWR | Boiling Water Reactor |
| CCTF | Cylindrical Core Test Facility |
| CFD | Computational Fluid Dynamics |
| CHF | Critical Heat Flux |
| DOE | Department of Energy |
| DP | Differential Pressure |
| ECC | Emergency Core Cooling |
| FOM | Figure of Merit |
| IET | Integral Effects Test |
| INKA | Integral Test Facility Karlstein |
| INL | Idaho National Laboratories |
| LDA | Laser doppler anemometry |
| LLD | Liquid Level Detectors |
| LOCA | Loss of Coolant Accident |
| LPP | Lagrangian Point Particle |
| LWR | Light Water Reactor |
| M&S | Modeling & Simulation |
| MSL | Main Steam Line |
| MSLB | Main Steam Line Break |
| MW | Megawatt |
| NCG | Non-Condensable Gas |
| NP | Not Provided |
| NPP | Nuclear Power Plant |
| NRC | Nuclear Regulatory Commission |
| POI | Phenomenon of Interest |
| PWR | Pressurized Water Reactor |
| RELAP | Reactor Excursion and Leak Analysis Program |
| RPV | Reactor Pressure Vessel |
| SCTF | Slab Core Test Facility |
| SET | Separate Effect Test |
| SGTR | Steam Generator Tube Rupture |
| SMR | Small Modular Reactor |
| TC | Thermocouple |
| UPTF | Upper Plenum Test Facility |
| V&V | Verification & Validation |
| VOF | Volume of Fluid |
| WMS | Wire-Mesh Sensor |

### Symbols

| | |
|---|---|
| m | meters |
| °C | degrees centigrade |
| J | joules |
| g | grams |
| s | second |
| $E_{fg}$ | entrainment amount |
| h | height above pool |
| j | superficial velocity |
| $\rho$ | density |
| $\Delta\rho$ | density difference between liquid and gas |
| $N_{\mu g}$ | gas viscosity number |
| $D_H$ | hydraulic diameter |
| SE | entrainment mass flux |
| $\mu$ | dynamic viscosity of the liquid |
| D | inner pipe diameter |
| We | Weber number |
| Re | Reynolds number |
| $\Gamma_E$ | entrainment rate |
| $V_E$ | entrained volume sub correlation |
| $\lambda_C$ | critical wavelength sub correlation |
| $\tau_C$ | characteristic time sub correlation |
| $y_x$ | constants |
| $\alpha$ | void fraction |
| $\alpha_T$ | temperature coefficient of resistance |
| $\sigma$ | conductance |
| I | radiation intensity |
| $\delta$ | film thickness |
| c | speed of sound at reference temperature |
| $t_\delta$ | time difference between interfaces |
| n | refractive index of optic material |
| v | velocity |
| p | pressure |
| $T_{Hot}$ | temperature being measured |
| $T_{Cold}$ | cold-junction temperature |
| $E_{emf}$ | voltage output of TC |
| S | Seebeck coefficient |
| R | resistance measured |
| T | temperature |
| $F_C$ | Coriolis force |
| w | angular velocity |
| x | tube length |
| f | vortex shedding frequency |
| d | bluff body width |
| St | Strouhal number |
| H | height |
| SG | specific gravity |
| D | distance |
| q | heat flux |

| Subscript/Superscript | |
|---|---|
| g | gas |
| chf | critical heat flux |
| * | dimensionless quantity |
| l | liquid |
| t | total |
| s | static |
| 0 | at 0 °C |

| | |
|---|---|
| t | time between transmission and detection |

| Prefix | |
|---|---|
| k | kilo |
| M | mega |
| μ | micro |
| m | milli |

## References


1. World Nuclear Association. Small Nuclear Power Reactors. Available online: https://www.world-nuclear.org/information-library/nuclear-fuel-cycle/nuclear-power-reactors/small-nuclear-power-reactors.aspx (accessed on 8 January 2024).
2. Bae, B.; Kim, T.; Kim, K.; Jeong, J.J.; Yun, B. Experimental investigation of droplet entrainment and deposition in horizontal stratified wavy flow. *Int. J. Heat Mass Transf.* **2019**, *144*, 118613. [CrossRef]
3. Kumar, S.; King, M.D. Numerical investigation on indoor environment decontamination after sneezing. *Environ. Res.* **2022**, *213*, 113665. [CrossRef] [PubMed]
4. Gulati, S. Simulation of Liquid Entrainment in BWR Annular Flow Using an Interface Tracking Method Approach. Doctoral Dissertation, Massachusetts Institute of Technology, Cambridge, MA, USA, 2012. Available online: https://dspace.mit.edu/bitstream/handle/1721.1/76966/824738893-MIT.pdf (accessed on 26 November 2024).
5. Ishii, M.; Grolmes, M.A. Inception criteria for droplet entrainment in two-phase concurrent film flow. *AIChE J.* **1975**, *21*, 308–318. [CrossRef]
6. Kataoka, I.; Ishii, M.; Mishima, K. Generation and size distribution of droplet in annular two-phase flow. *J. Fluids Eng.* **1983**, *105*, 230–238. [CrossRef]
7. FluidFlow. Flow Regime in Two-Phase Liquid-Gas Flow. Available online: https://blog.fluidflowinfo.com/two-phase-liquid-gas-flow-regime (accessed on 8 January 2024).
8. Hewitt, G.F. Gas-Liquid Flow. Begel House Inc. Available online: https://www.thermopedia.com/content/2/ (accessed on 8 January 2024).
9. Entry, E.B. Steam Tables. Thermopedia. Available online: https://www.thermopedia.com/content/1150/ (accessed on 8 January 2024).
10. Troitskaya, Y.; Kandaurov, A.; Ermakova, O.; Kozlov, D.; Sergeev, D.; Zilitinkevich, S. Bag-breakup fragmentation as the dominant mechanism of sea-spray production in high winds. *Sci. Rep.* **2017**, *7*, 1614. [CrossRef]
11. Lecoeur, N. Interfacial Behaviour in Stratified and Stratifying Annular Flows. Doctoral Dissertation, Imperial College London, London, UK, 2013.
12. Pham, S.H.; Kawara, Z.; Yokomine, T.; Kunugi, T. Detailed observations of wavy interface behaviors of annular two-phase flow on rod bundle geometry. *Int. J. Multiph. Flow* **2014**, *59*, 135–144. [CrossRef]
13. Thome, J.R.; Cioncolini, A. Entrained liquid fraction in annular two-phase flow. In *Encyclopedia of Two-Phase Heat Transfer and Flow I: Fundamentals and Methods*; World Scientific: Singapore, 2015; pp. 113–142.
14. Zhang, P.; Chen, P.; Li, W.; Di, Z.; Zhang, L.; Hu, X.; Zou, Y. An experimental study of pool entrainment in high gas flux region. *Prog. Nucl. Energy* **2016**, *89*, 191–196. [CrossRef]
15. Zhang, P.; Li, W.; Di, Z.; Hu, X.; Chen, L.; Chang, H.; Chen, P. An experimental study of pool entrainment with side exit. *Ann. Nucl. Energy* **2017**, *110*, 406–411. [CrossRef]
16. Wright, R.F.; Terry, L.S.; Jose, N.R.; John, G. Characterization of Liquid Entrainment in the AP1000 Automatic Depressurization System from APEX Tests. 2005. Available online: https://www.osti.gov/etdeweb/biblio/20735022 (accessed on 26 November 2024).
17. Welter, K.; Bajorek, S.; Reyes, J., Jr.; Woods, B.; Groome, J.; Hopson, J.; Young, E.; DeNoma, J.; Abel, K. *APEX-AP1000 Confirmatory Testing to Support AP1000 Design Certification (Non-Proprietary), NUREG-1826*; United States Nuclear Regulatory Commission: Washington, DC, USA, 2005. Available online: https://www.nrc.gov/docs/ML0529/ML052980061.pdf (accessed on 26 November 2024).
18. Sun, D.; Xiang, Y.; Tian, W.; Liu, J.; Zhang, P.; Qiu, S.; Su, G. Experimental investigation of upper plenum entrainment in AP1000. *Prog. Nucl. Energy* **2015**, *80*, 80–85. [CrossRef]
19. Henry, F. Experimental and Modeling Investigations on Droplet Entrainment in a PWR Hot Leg Under Stratified Flow Conditions. Ph.D. Dissertation, Université Catholique de Louvain, Ottignies-Louvain-la-Neuve, Belgium, 2016. Available online: http://hdl.handle.net/2078.1/178058 (accessed on 26 November 2024).
20. Ouallal, M.; Leyer, S.; Gupta, S. A correlation for pool entrainment phenomenon. *Nucl. Eng. Des.* **2021**, *383*, 111386. [CrossRef]
21. Pan, L.; Hanratty, T.J. Correlation of entrainment for annular flow in horizontal pipes. *Int. J. Multiph. Flow* **2002**, *28*, 385–408. [CrossRef]
22. Damerell, P.S.; Simons, J.W. *2D/3D Program Work Summary Report, [January 1988–December 1992]*; US Nuclear Regulatory Commission (NRC): Washington, DC, USA, 1993. [CrossRef]

23. Leyer, S.; Wich, M. The integral test facility Karlstein. *Sci. Technol. Nucl. Install.* **2012**, *2012*, 47071301. [CrossRef]
24. Fossum, K.; Bhowmik, P.K.; Sabharwall, P. Uncertainty Propagation from Experiment Measurements to Modeling Approaches: A Case for SMR Steam Entrainment Testing. In Proceedings of the 2024 International Congress on Advances in Nuclear Power Plants (ICAPP), Las Vegas, NV, USA, 16–19 June 2024. Available online: https://inl.elsevierpure.com/en/publications/uncertainty-propagation-from-experiment-measurements-to-modeling- (accessed on 26 November 2024).
25. Tompkins, C.; Prasser, H.-M.; Corradini, M. Wire-mesh sensors: A review of methods and uncertainty in multiphase flows relative to other measurement techniques. *Nucl. Eng. Des.* **2018**, *337*, 205–220. [CrossRef]
26. Entry, E.B. Void Fraction Measurement. Thermopedia. Available online: https://www.thermopedia.com/content/281/ (accessed on 8 January 2024).
27. Ofuchi, C.Y.; Eidt, H.K.; Bertoldi, D.; Da Silva, M.J.; Morales, R.E.; Neves, F. Void Fraction Measurement in a Gas-Liquid Swirling Flow Using an Ultrasonic Sensor. *IEEE Access* **2020**, *8*, 194477–194484. Available online: https://ieeexplore.ieee.org/stamp/stamp.jsp?arnumber=9237984 (accessed on 26 November 2024). [CrossRef]
28. Stankovic, B. An Experimental Study on the Local Void Fraction Measurements in Large-Diameter Vertical Pipes Using Optical Fiber Probes. Doctoral Dissertation, McMaster University, Hamilton, ON, Canada, 1997. Available online: https://macsphere.mcmaster.ca/bitstream/11375/25562/1/Stankovic_Branko_1997Aug_Masters.pdf (accessed on 26 November 2024).
29. Benson, T. Pitot Tube. National Aeronautics and Space Administration. Available online: https://www.grc.nasa.gov/www/k-12/VirtualAero/BottleRocket/airplane/pitot.html (accessed on 8 January 2024).
30. OMEGA Engineering, Inc. Cold Junction Compensation for Thermocouples. Available online: https://www.omega.com/en-us/resources/thermocouple-junction-principles (accessed on 8 January 2024).
31. Instrumentation Toolbox. Basics of Resistance Temperature Detectors (RTDs). Available online: https://www.instrumentationtoolbox.com/2011/01/sensors-used-in-industrial_23.html (accessed on 26 November 2024).
32. OMEGA Engineering, Inc. Coriolis Mass Flow Meters. Available online: https://www.omega.co.uk/prodinfo/coriolis-flow-meter.html (accessed on 8 January 2024).
33. OMEGA Engineering, Inc. What Is a Vortex Flow Meter? Available online: https://www.omega.com/en-us/resources/vortex-flow-meter (accessed on 8 January 2024).
34. Yokogawa. Differential Pressure Level Solutions. Yokogawa Electric Corporation. Available online: https://web-material3.yokogawa.com/BU01C25A04-01EN-Y_002.pdf (accessed on 8 January 2024).
35. Indumart Inc. Various Technics of Liquids and Solids Level Measurements (Part 4). Available online: https://indumart.com/Level-measurement-4.pdf (accessed on 8 January 2024).
36. Zhao, A.; Han, Y.-F.; Ren, Y.-Y.; Zhai, L.-S.; In, N.-D. Ultrasonic method for measuring water holdup of low velocity and high-water-cut oil-water two-phase flow. *Appl. Geophys.* **2016**, *13*, 179–193. [CrossRef]
37. NASA. Navier-Stokes Equations. National Aeronautics and Space Administration. Available online: https://www.grc.nasa.gov/www/k-12/airplane/nseqs.html (accessed on 8 January 2024).
38. Flow Science, Inc. Lagrangian Particles. Available online: https://www.flow3d.com/resources/cfd-101/general-cfd/lagrangian-particles/ (accessed on 8 January 2024).
39. Chaussonnet, G.; Dauch, T.; Keller, M.; Okraschevski, M.; Ates, C.; Schwitzke, C.; Koch, R.; Bauer, H.-J. Progress in the smoothed particle hydrodynamics method to simulate and post-process numerical simulations of annular airblast atomizers. *Flow Turbul. Combust.* **2020**, *105*, 1119–1147. [CrossRef]
40. Afolabi, E.A.; Lee, J. An eulerian-eulerian CFD simulation of air-water flow in a pipe separator. *J. Comput. Multiph. Flows* **2014**, *6*, 133–149. [CrossRef]
41. Khan, I.; Wang, M.; Basit, M.A.; Tian, W.; Su, G.; Qiu, S. CFD modeling of liquid entrainment through vertical T-junction of fourth stage automatic depressurization system (ADS-4). *Ann. Nucl. Energy* **2021**, *159*, 108317. [CrossRef]
42. Singh, D.; Das, A.K. Predictability and benefits of coupled Eulerian-Lagrangian approach over Eulerian characterization of droplet annular flow. *Fluid Dyn. Res.* **2021**, *53*, 065501. Available online: https://iopscience.iop.org/article/10.1088/1873-7005/ac34ec/pdf (accessed on 26 November 2024). [CrossRef]
43. Li, L.; Li, B. Investigation of bubble-slag layer behaviors with hybrid Eulerian–Lagrangian modeling and large eddy simulation. *J. Manag.* **2016**, *68*, 2160–2169. [CrossRef]
44. Kumar, S.; Klassen, M.; Klassen, D.; Hardin, R.; King, M.D. Dispersion of sneeze droplets in a meat facility indoor environment—Without partitions. *Environ. Res.* **2023**, *236*, 116603. [CrossRef] [PubMed]
45. Song, G.; Zhang, D.; Liu, Q.; Xiang, Y.; Su, G.H.; Tian, W.; Qiu, S. RELAP5/MOD3.4 calculation and model evaluation based on upper plenum entrainment experiment in AP1000. *Ann. Nucl. Energy* **2020**, *138*, 107143. [CrossRef]
46. Vuong, D.H.; Sarica, C.; Pereyra, E.; Al-Sarkhi, A. Liquid droplet entrainment in two-phase oil-gas low-liquid-loading flow in horizontal pipes at high pressure. *Int. J. Multiph. Flow* **2018**, *99*, 383–396. [CrossRef]
47. Lopes, J.; Dukler, A. Droplet entrainment in vertical annular flow and its contribution to momentum transfer. *AIChE J.* **1986**, *32*, 1500–1515. [CrossRef]


**Disclaimer/Publisher's Note:** The statements, opinions and data contained in all publications are solely those of the individual author(s) and contributor(s) and not of MDPI and/or the editor(s). MDPI and/or the editor(s) disclaim responsibility for any injury to people or property resulting from any ideas, methods, instructions or products referred to in the content.